Extensive Cavitation Tunnel Acoustic Characterization of Controllable Pitch Propellers

F. MIGLIANTI[a,1], G. TANI[a], M. VIVIANI[a], D. BERTETTA[b] and C. VACCARO[b]
[a] *DITEN–University of Genoa, Genoa, Italy*
[b] *Fincantieri C.N.I –Naval vessel business unit, Genoa, Italy*

Abstract. Experimental tests in model-scale are the currently established (and more reliable) methods for the propeller acoustic characterization. However, they are affected by uncertainties mostly due to scale effects, which make it difficult to consistently reproduce in model-scale some of full-scale functioning conditions.

In order to cope with this issue, it is interesting to define empirical formulations to shape the most significant cavitating phenomena in terms of underwater radiated noise spectrum. A suitable approach for the determination of such formulations may consist in the experimental characterization of model propellers collecting a large amount of data such to accurately describe propeller functioning conditions and related noise emissions. Collected data should be then analysed to extrapolate desired formulations exploiting advanced data analysis techniques.

In the present work the acoustical characterization of two propellers, performed at the University of Genoa cavitation tunnel, is presented. The collected sample includes cavitation buckets with inception points of different phenomena, noise spectra, pressure pulses and photos picked up at various pitches and functioning points, including off design conditions.

Keywords. cavitation, radiated noise, CP propellers

1. Introduction

The attention to underwater acoustic radiation is not a new topic of research, but if in the past it concerned mainly naval vessels, nowadays the increasing attention to environmental issues [1] and comfort on board [2], gives the opportunity to spread the practical applications of these studies. Among the various sources of underwater radiated noise [3], the cavitating propeller is commonly the dominant one.

Propeller noise assessment during the design stage mainly relies on semi empirical formulations and model-scale experiments, commonly carried out in cavitation tunnels. However, scale effects [4] may affect model-scale tests, producing results not fully consistent with the behavior of full-scale propeller. As it is well known, different cavitation phenomena are subject to different scaling rules hence equal kinematic condition and cavitation index, between full and model-scale, do not lead necessarily to the same cavitation pattern in the propeller. Consequently, noise spectra could be

[1] Fabiana Miglianti, Corresponding author, DITEN Department, Genoa University, Via Montallegro 1, 16145-Genova, Italy; E-mail: fabiana.miglianti@edu.unige.it.

inconsistent with the full-scale propeller acoustic; in particular the noise produced by the expected full-scale cavitation pattern can be masked or altered by the co-existence of other not consistent phenomena [5]. On the other hand, model-scale facilities offer the opportunity to analyze cavitation noise for a large variety of combinations of different phenomena, hence providing a large amount of data to characterize cavitation noise.

Data-based models may allow to extract phenomena explanations with none knowledge a priori [6] of the mathematical rules governing them, hence they could represent an effective tool to exploit model-scale results with the aim to extrapolate spectral characteristics of those cavitation phenomena which in some cases cannot be correctly reproduced in model-scale. With a view to the development of data driven models for the prevision of underwater radiated noise from cavitating propellers, a collection of cavitation tests was performed and is here outlined.

2. Experimental Set Up

The tests were carried out at the UNIGE cavitation tunnel, the facility is a Kempf & Remmers K22 closed circuit tunnel with a testing section of 0.57 m × 0.57 m, long 2 m. Thrust, torque and revolution rate of the propeller are measured by a Kempf & Remmers H39 dynamometer. Cavitation is visualized with a stroboscope and two hand lamps, while photos are taken with three Allied Vision Tech Marlin F145B2 Firewire cameras, with a resolution of 1392×1040 pixels. The index of the susceptibility of water to cavitation in current tests is dissolved oxygen content, which is measured by an ABB sensor model 8012/170.

The tunnel is equipped with a laser doppler velocimetry system by Spectra-Physics for detailed non-intrusive flow measurements. Propeller noise measurements are picked up with two hydrophones (namely a Bruel & Kjaer 8103 and a Reson TC4013), connected to two Bruel & Kjaer 2635 amplifier. For pressure pulses surveys five differential Kulite XTL-190M-5G transducers were used. All the tests were performed in accordance with ITTC 2017 guidelines [5].

The inflow wake was modeled reproducing in the tunnel the nominal wake field measured in towing tank (neglecting voluntarily the possible difference of the full-scale wake). To this aim, a small dummy model is used to reproduce approximately a typical twin-screw ship wake field. Then axial components are adjusted with the help of suitably built wake screens attached to the dummy. Finally, since the main transversal flow component is vertical upward, propeller shaft is inclined so to reproduce such component. Adopted inclinations are 6.8° for propeller A and 2.5° for B and 2B. In Figure 1 propeller A configuration is reported.

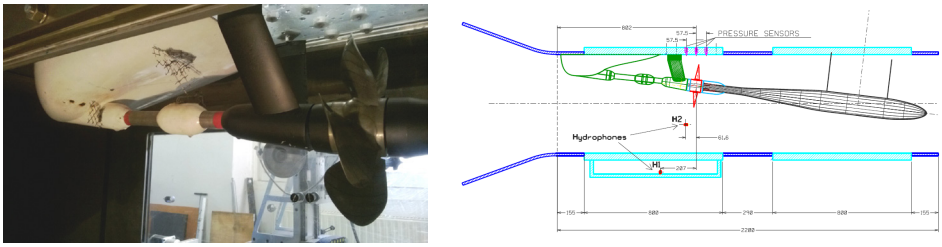

Figure 1. Propeller A, dummy model and wake screens (left) and set up overview (right).

The oxygen amount is set between the 40% and 50% of its saturated value at atmospheric pressure. Radiated noise measurements were carried out with one hydrophone mounted on a small cylindrical support protruding from a fin immersed in the tunnel flow, outside the propeller slipstream. The other hydrophone is located inside a tank full of water attached to the Plexiglas window under the propeller. The five pressure sensors are mounted on the Plexiglas window just above the propeller.

Measurements were carried out mainly with a shaft rate equal to 25 rps. Lower rotational rates (22.5 or 20 rps) were adopted when necessary to avoid exceeding dynamometer maximum allowed loads. Propeller loading conditions were defined according to the identity of the thrust coefficient K_T and the cavitation number based on rotational speed σ_N. In the following the procedure adopted for noise tests and post processing is shown. For the sake of shortness, results of the tests on only one propeller are shown in this work, however the same procedure has been adopted for all test cases.

2.1. Cavitation Noise Measurements

The noise measurements performed for each point are repeated in different days, allowing to collect a series of repeated tests (usually from four to six), to assess measurements repeatability and to analyze intermittency problems which may affect cavitation inception and extension. Such issues may be due to the lack of cavitation nuclei concentration and distribution (and related direct measurement). Every repetition has been performed at constant DO_2, being the dissolved oxygen the only index of the susceptibility to cavitation available for current campaign. To facilitate comparisons between noise levels, pressure signals are reported in terms of non-dimensional pressure coefficient K_P.

The background noise is measured replacing the propeller with a dummy hub and running the tunnel at the same operational conditions. The net noise is the contribution to the total noise due only to the cavitation and propeller functioning. According to ITTC guidelines, net noise levels are calculated by means of a logarithmic subtraction of the background noise to the total one. This applies for frequencies where the signal to noise ratio is larger or equal to 3 dB, otherwise the measure is discarded.

Finally, net noise levels are normalized with respect to the distance between the sensor and acoustical center of the propeller. For present study this has been defined in correspondence to the center of the propeller disk. Transfer function corrections for the confined environment effects have not been applied.

3. Test Cases

As anticipated two CP propellers were considered in the present campaign, whose main characteristics are reported in Table 1. Propeller A and B were tested in correspondence to various pitches and both were mounted in pulling configuration to better control inflow characteristics. Propeller 2B is just the same as B but mounted in pushing condition to perform the characterization of the hub vortex cavitation, thus deviating from the main configuration described in previous section. The dummy model was not present in this case resulting in completely different inflow conditions. Actually, in this case the axial wake field is represented only by the weak disturbances coming from the inclined dynamometer and the shaft brackets.

Table 1. Model propellers characteristics.

	Propeller A	**Propeller B**	**Propeller 2B**
Number of blades	5	5	5
Diameter [m]	0.25	0.25	0.25
Direction of rotation	Right	Right	Right
Design pitch ratio at 0.7R	1.156	1.385	1.385
Reduced (-3°) pitch ratio at 0.7R	1.013	1.229	
Reduced (-5°) pitch ratio at 0.7R	0.938		
Reduced (-6°) pitch ratio at 0.7R		1.082	
Incremented (+2°) pitch ratio at 0.7R	1.256		

For each pitch setting, tests include: cavitation bucket, cavitation extension, photographs in correspondence to different functioning conditions, pressure pulses and propeller radiated noise measurements in a large set of operational conditions. This set of points were defined with the aim of providing data for future analyses. Due to this, operational conditions include many off-design conditions not corresponding to any real functioning condition of the ship.

Measuring points are defined to characterize propeller noise considering different cavitation typologies at different stages of development, regardless of their significance for the ship functioning. An example of noise measuring points set can be seen together with the cavitation bucket in Figure 2. In general, a proper set of loading conditions in terms of thrust coefficients K_T is considered, distributed around those values corresponding to real functioning points of the ship. For each value of the thrust coefficient, different values of the cavitation number are considered for tests.

Cavitation number values are defined ranging from the one corresponding to atmospheric pressure (with cavitation suppression or very limited cavitation) to one characterized by very low undisturbed pressure, so to explore different cavitating regimes, from no cavitation (if possible) to fully developed cavitation. The lower limit for the cavitation index is given by those values for which the cavitation pattern is no more realistic, typically characterized by the presence of considerably extended bubble cavitation, whose acoustical characterization is not within the aims of present research.

Therefore, the effects of the overall phenomenon on noise can be analyzed in its different stages of development. It must be considered that, obviously, the presence of only one type of cavitation is very rare. Also due to this, even significantly off design K_T values are of interest because moving away from design conditions certain types of cavitation are stronger and so they can be better isolated and studied in further analyses. In total almost 500 different spectral noise were picked up, almost equally subdivided among all the pitches.

4. Noise Survey Results

In the following the results for Propeller A at design pitch are shown. In Figure 2 the measuring points are reported directly on the cavitation bucket. Actual values of cavitation number and thrust coefficient are not reported in the figure for the sake of confidentiality.

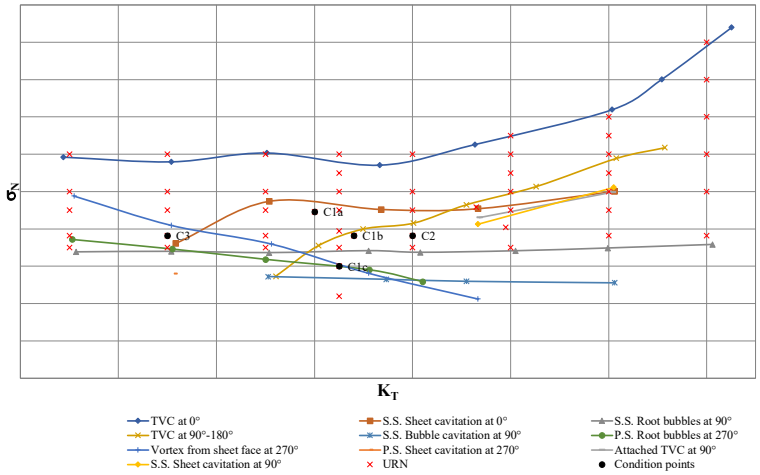

Figure 2. Propeller A cavitation bucket.

A subset of points, listed in detail in Table 2, will be considered in present work in order to qualitatively analyse collected data and observable trends. The points are chosen among those whose photographs are available, with interesting cavitation phenomena. For these tests, the shaft rotational speed is fixed at 25 rps. Non-dimensional thrust K_T and cavitation index σ_N are indicated in percentage with respect to the reference condition C1b, in the third column a brief description of the cavitation types detected is reported.

Table 2. Test cases conditions at model-scale.

Propeller condition	%K_T	%σ_N	Cavitation types
C1a	95	117	Tip Vortex Cavitation at 0°, Suction Side sheet at 0°
C1b	100	100	Same as C1a plus TVC at 90°-180° (inception)
C1c	98	79	Same as C1b plus Vortex From Sheet Face at 270° (inception), root bubbles on S.S. at 90° and on Pressure Side at 270° (inception)
C2	107	100	Same as C1b
C3	77	100	TVC at 0° and VFSF at 270°

In Table 3 the images of cavitation patterns from three different views are reported.

Table 3. Cavitation photographs at test cases conditions.

Suction side cavitation at 0°	Suction side cavitation at 90°	Pressure side cavitation at 270°
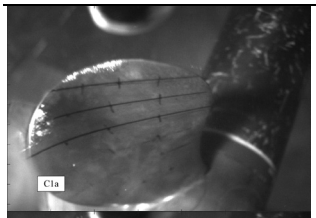	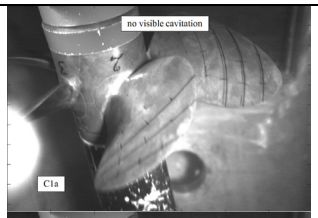	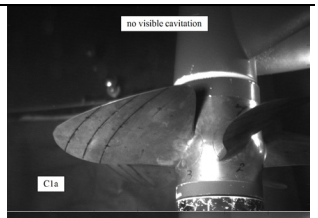
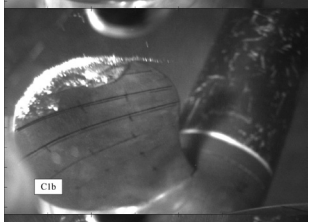	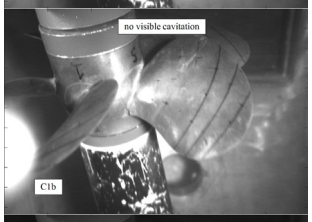	
		
		
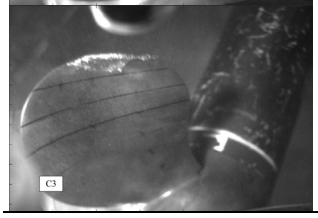	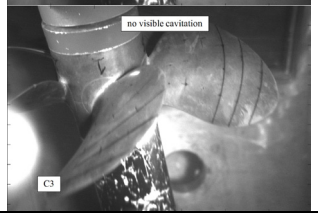	

Conditions C1a, C1b and C1c have almost the same propeller load but the cavitation index decreases from a to c; they are affected by tip vortex cavitation at 0° and suction side sheet cavitation at 0°. Both phenomena are highly nonstationary due to the presence of non-uniform inflow wake. The cavitation pattern, especially sheet cavitation, varies significantly depending on the blade position. S.S. sheet cavitation is larger moving from C1a to C1c because of smaller σ/σ_i[2] ratio. Tip vortex increases in strength and size from C1a to C1c and it gets visible for a wider range of blade angular positions, also outside the wake peak. Condition C2 is at the same cavitation index of C1b but with a more loaded propeller: as a consequence, cavitation phenomena

[2] This quantity is defined as the ratio between the current cavitation index and the inception one of the phenomenon. It can be used as an indication of the intensity of cavitation.

occurring on the suction side are stronger, as it can be seen by the photo at 90° where the presence of a more marked tip vortex is clearly visible. The last test case, C3, is located at the same cavitation index of C1b and C2 but with a lower thrust coefficient; this lead, obviously, to weaker cavitation phenomena on the suction side and stronger on the pressure side, namely the VFSF. As visible in the cavitation bucket, suction side root bubbles inception occurs at rather low cavitation number and it is only slightly influenced by the variation of blades load experienced for the wide range of K_T considered. Among the functioning points considered in present work, bubble cavitation is present only for C1c at the suction side root of the blades at 90°. In the same condition, also pressure side root bubbles are present even if not visible in the photographs (inception point). Figure 3 reports the spectra of net noise levels referred at 1 meter from the propeller disk centre, relative to the hydrophone inside the tunnel flow; the spectra show a signal to noise ratio greater than 3 dB for nearly all the frequencies.

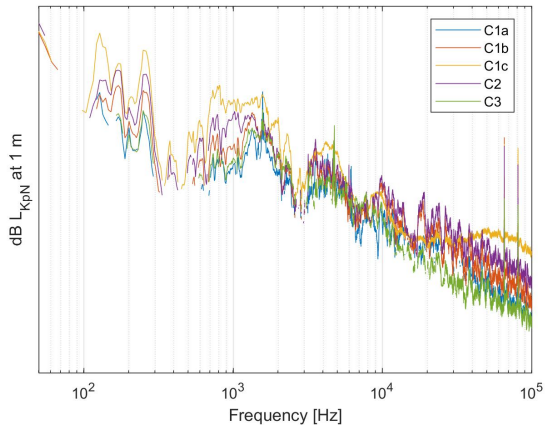

Figure 3. Net noise spectra normalized at 1 meter.

Typically, the hump visible at around 1.500 Hz for C1b is linked to the cavitating tip vortex; this, as known, tends to shift towards lower frequencies and increase in amplitude when the vortex increases in radius. This happens in correspondence to those conditions where the TVC is stronger due to lower σ_N (C1c) or where the K_T is larger (C2), hence when the vortex cavitation is more severe. The opposite occurs when the vortex becomes weaker, as in C1a and C3. Considering the two conditions in which vortex extension is higher (C1c and C2), it is clear that the vortex peak is not well defined, being distributed on a larger frequency range. This may be attributed to the vortex diameter variation during the blade revolution and consequently a nonstationary vortex pulsation frequency. Moreover, in these cases also intense S.S. sheet cavitation is present (especially in condition C1c), with strong interaction (bursts) with the wake peak. The high frequency spectrum, from TVC frequency to 100 kHz, is usually ruled by sheet and (more influent when present) bubble cavitation. As it can be seen, point C1c is the only one featuring bubble cavitation; consequently, much higher power levels are present.

5. Conclusions

Two controllable pitch propellers in correspondence to various pitch configurations have been tested. Underwater radiated noise spectra show typical behaviors according to the typology, extension, location and strength of the cavitation phenomena. Hence collected data may be reasonably used to identify and model such typical trends.

Given the objective difficulty to define analytical formulations, semi-empirical formulations [7][8] and data-driven algorithm can be helpful to extract spectral information (e.g. tip vortex central frequency and amplitude) from the measured points, with the final aim of predicting them for cases not directly tested in the cavitation tunnel. This could allow to forecast propeller noise also for those full-scale conditions for which, because of viscous scale effects, it is difficult or even not possible, to reproduce cavitation similarity in model-scale. Indeed, the presence of sheet and bubble cavitation at model-scale can mask or alter the noise produced by the vortex cavitation, like for test condition C1c, being usually the latter the only one expected in full-scale trials.

The future steps of the ongoing activity will be the definition of a simplified and generalized spectral form to reduce drastically the number of spectral frequencies without losing information, with the aim of facilitating the following data analysis.

Then a detailed feature analysis will be carried out, in order to study the influence of the various variables, taken individually or by their combinations, affecting cavitation noise and to select the most influent. Finally, specific algorithm, trained on the resultant test data, will be used to extrapolate the tip vortex spectral noise for those function points that cannot be reproduced consistently in model-scale.

References

[1] Merchant N.D., Pirotta E., Barton T.R., Thompson P.M., Monitoring ship noise to assess the impact of coastal developments on marine mammals, *Marine Pollution Bulletin* **Vol.78** (2014), 85–95.

[2] ISO 20283–5:2016, *Measurement of vibration on ships–Part 5: Guidelines for measurement, evaluation and reporting of vibration with regard to habitability on passenger and merchant ships*, International Organization for Standardization, Geneva, 2016.

[3] Ross D., *Mechanics of Underwater Noise*, Pergamon Press, Oxford, 1976.

[4] Bark G., Prediction of propeller cavitation noise from model tests and its comparison with full-scale data, *Journal of Fluids Engineering* **Vol.107** (1985), 112–120.

[5] ITTC Recommended procedures and guidelines, *Model–scale propeller cavitation. Noise measurements*, 7.5–02–01–05, 2017.

[6] Vapnik V.N., *Statistical learning theory*, Wiley–Interscience, New York, 1998.

[7] Bosschers J., Investigation of hull pressure fluctuations generated by cavitating vortices, *First International Symposium on Marine Propulsors, smp'09*, Trondheim, Norway, (2009).

[8] Raestad, A.E., Tip vortex index–an engineering approach to propeller noise prediction, *The Naval Architect* (July/August 1996), 11–16.